Quantitative determination of the atomic scattering tensor in orbitally ordered $YTiO_3$ by using a resonant x-ray scattering technique

H. Nakao,[1,2,*] Y. Wakabayashi,[1,3] T. Kiyama,[1,†] Y. Murakami,[1,2,*] M. v. Zimmermann,[4,‡] J. P. Hill,[4] Doon Gibbs,[4] S. Ishihara,[5,*] Y. Taguchi,[5,§] and Y. Tokura[5,6]

[1]*Photon Factory, Institute of Materials Structure Science, High Energy Accelerator Research Organization (KEK), Tsukuba, 305-0801, Japan*

[2]*CREST, Japan Science and Technology Corp., Tsukuba, 305-0045, Japan*

[3]*Department of Physics, Keio University, Yokohama 223-8522, Japan*

[4]*Department of Physics, Brookhaven National Laboratory, Upton, New York 11973-5000*

[5]*Department of Applied Physics, University of Tokyo, Tokyo 113-8656, Japan*

[6]*Joint Research Center for Atom Technology (JRCAT), Tsukuba, 305-0046, Japan*

(Received 17 July 2002; published 18 November 2002)

The orbitally ordered state of $YTiO_3$ has been investigated utilizing resonant x-ray scattering (RXS) near the Ti *K*-edge. The RXS intensities have been observed at the $1s \rightarrow 4p$ dipole transition energy (the main edge). The atomic scattering tensor of the Ti ion has quantitatively been determined by measurements of the azimuthal angle and polarization dependence of the signal at several scattering vectors. On the basis of the tensor, we discuss not only the scattering mechanism but also the wave function of the orbitally ordered state, finding it to be a linear combination of two t_{2g} orbitals. In addition, RXS at the $1s \rightarrow 3d$ transition energy (the pre-edge) was also observed. This signal was found to have the same azimuthal angle and polarization dependence as that at the main edge.

DOI: 10.1103/PhysRevB.66.184419 PACS number(s): 71.30.+h, 61.10.Eq, 71.27.+a

I. INTRODUCTION

In addition to the charge and spin degrees of freedom, the orbital degree of freedom plays an important role in determining the electric and magnetic properties of the perovskite transition-metal oxides. However, experimental techniques to observe orbital ordering have been limited to date. In recent years, the study of orbital ordering utilizing a resonant x-ray scattering (RXS) technique has been rapidly developed. In particular, the orbital ordering of the e_g electron of Mn^{3+} in some manganites has been observed by this technique.[1–5] RXS at the $1s \rightarrow 4p$ dipole transition energy of a Mn ion is caused by a splitting in the Mn $4p$ orbital energy levels as a result of the orbital ordering.[6–8] Two possible scenarios for this lifting of the degeneracy of the Mn $4p$ orbitals have been proposed. The first is a Coulomb interaction between the Mn $3d$ and $4p$ orbitals (the Coulomb mechanism).[6] The second is an anisotropic hybridization of the Mn $4p$ with the neighboring O $2p$, resulting from the distortion of the oxygen octahedra, that is the Jahn-Teller distortion (JTD) (the JT mechanism).[7,8] It remains controversial as to which of these mechanisms is more significant in giving rise to RXS. In either case, however, the RXS signal provides information on the orbital ordering, and the orbitally ordered state can be characterized using the RXS technique without a full structural analysis. Moreover, the correlation length of orbitally ordered state can be measured by this technique,[4,5] and RXS studies have now been extended to other materials, e.g., YVO_3,[9] $LaTiO_3$,[10] DyB_2C_2,[11] and CeB_6.[12]

The e_g-electron systems such as the manganites exhibit a strong electron-lattice coupling due to the hybridization between the O $2p$ orbital and the Mn e_g orbital, that is, they exhibit a large JTD. On the other hand, t_{2g}-electron systems have a weak electron-lattice coupling (small JTD). As a result, it is expected that the JT mechanism in a t_{2g} system is less effective in giving rise to RXS than that in an e_g system. Thus studies of such systems may give insight into the question of which mechanism of RXS is the dominant one.

$YTiO_3$ is an example of a t_{2g} electron system. It is a ferromagnetic insulator ($T_c \sim 30$ K) having an orthorhombic space group $Pbnm$ ($GdFeO_3$-type structure) with lattice constants $a = 5.316$ Å, $b = 5.679$ Å, and $c = 7.611$ Å.[13] The crystal structure has a JTD in which the Ti-O distances are Ti-$O_x \sim 2.08$ Å, Ti-$O_y \sim$ Ti-$O_z \sim 2.02$ Å at site 1. Because of the longest Ti-O distance along the x axis, the xy and zx of the t_{2g} orbital are stabilized, namely, two degenerate orbitals are occupied by one electron. However, because of the Coulomb interaction among the t_{2g} orbitals and/or the crystal structure, this orbital degeneracy is lifted. The orbitally ordered state of the $3d$ electron of the Ti^{3+} ion is well studied by both theory[14,15] and experiment.[16,17] Theoretical calculations using unrestricted Hartree-Fock calculation[14] and generalized gradient approximation[15] predict the wave functions of orbitally ordered state to be linear combination of two t_{2g} orbitals at sites 1–4, as shown in Fig. 1. Ichikawa *et al.* have directly determined the wave function of the ordered orbital from the spin-density distribution by using the polarized neutron-scattering technique.[16] In addition, Ito *et al.* have determined the wave function based on a ^{47,49}Ti NMR experiment.[17] Both experimental results are consistent with the theoretical predictions as shown in Table I. However, these techniques are limited to the observation of the orbital ordering when accompanied by magnetic ordering, namely, the techniques can only determine the orbitally ordered state below T_c.

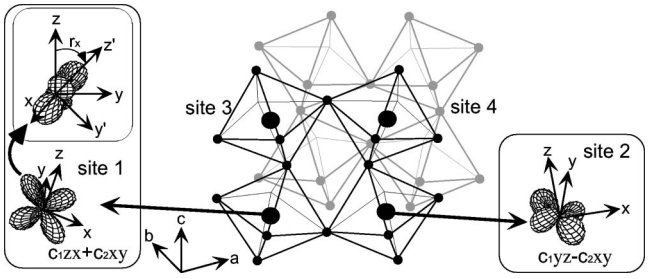

FIG. 1. Crystal structure of $YTiO_3$ with the $GdFeO_3$-type distortion. There are four Ti atoms in the unit cell, numbered 1–4, which are located at $(0,\frac{1}{2},0)$, $(\frac{1}{2},0,0)$, $(0,\frac{1}{2},\frac{1}{2})$, and $(\frac{1}{2},0,\frac{1}{2})$, respectively. The wave functions at sites 1–4, are c_1zx+c_2xy, c_1yz-c_2xy, c_1zx-c_2xy, and c_1yz+c_2xy. The *x*, *y*, and *z* axes are taken along the directions of Ti-O in the TiO_6 octahedron. The inset of site 1 shows an alternate coordinate system with the axes aligned with the orbital, namely, the $xy'z'$ coordinates are defined as the xz' plane in which the t_{2g} orbital is elongated. The angle between the *z* and z' axes following a rotation about the *x* axis is defined as r_x.

In $YTiO_3$, we have studied the RXS at the forbidden reflections near the Ti *K*-edge energy. The atomic scattering factor (ASF) tensor of the Ti ion at room temperature ($>T_c$) was determined from measurements of the azimuthal angle, polarization, and *Q*-position dependence of the RXS intensities at $1s\rightarrow 4p$ dipole transition energy. The anisotropy of the tensor is consistent with our model calculation for a $4p$ orbital polarization that arises from the on-site Coulomb interaction between the Ti $3d$ and $4p$ (i.e., the Coulomb mechanism). From the point of view of this Coulomb mechanism, we have succeeded in determining the wave function of the ordered orbital quantitatively, obtaining good agreement with the results of previous theories and experiments below T_c. Our data of the RXS are also compared with some other recent theories.[18,19] The other contributions to RXS, which are not included in the present analysis, such as the the tilting of neighboring oxygen octahedrons, are discussed. More detailed theoretical calculation is desired to understand this RXS mechanism. At the $1s\rightarrow 3d$ transition energy (pre-edge), RXS, which is expected theoretically to directly reflect the neighboring $3d$-orbital states, was also observed. The azimuthal angle, polarization, and *Q*-position dependence of the RXS at the pre-edge was the same as that at the main edge. The temperature dependence of the RXS shows no anomaly at the ferromagnetic transition temperature (T_c), although magnetostriction was observed.

II. EXPERIMENT

The single crystals used in this study were grown by a floating-zone technique. (100), (001), and (011) surfaces were cut and polished with fine emery paper and diamond paste. The full width at half maximum of the typical mosaic width was 0.07°. X-ray scattering experiments were carried out at beam line X22C at the National Synchrotron Light Source (BNL). The incident beam was monochromatized by a pair of Ge(111) crystals, giving an energy resolution of about 5 eV, and focused by a bent cylindrical mirror. Polarization analysis of the scattered beam was performed using a PG(004) analyzer crystal, which gives a scattering angle of 96.0° when the incident photon energy is set to the Ti *K*-edge. The incident polarization was about 95% linearly polarized in the horizontal plane; that polarization vector is σ. The polarization vector, σ' (π'), of scattered beam is perpendicular (parallel) to the scattering plane. The azimuthal angle and energy dependence of the RXS were studied at room temperature. For low-temperature experiment, the sample was mounted in a closed cycle He cryostat.

III. EXPERIMENTAL RESULTS AND DISCUSSIONS

A. Energy dependence

Near the Ti *K*-edge, the fluorescence of $YTiO_3$ was measured at (0,0,1.5) as shown in Fig. 2(a). There are two large peaks at $E=4.974$ (main edge) and 4.988 KeV of the $1s\rightarrow 4p$ dipole transition energy. This energy spectrum is similar to that of $LaMnO_3$ at Mn *K*-edge (Ref. 2: Fig. 2). Moreover, the fluorescence intensity shows a small shoulder at $E\sim 4.962$ keV (pre-edge) which corresponds to the $1s\rightarrow 3d$ quadrupole transition energy.

The energy dependence of the RXS intensity was measured at the forbidden reflections, (1 0 0), (0 0 1), and (0 1 1), where the observation of the RXS owing to the orbital ordering is expected. To avoid contamination due to multiple scattering, the energy dependence was measured at several azimuthal angles. The data, free of multiple scattering, are shown in Fig. 2. Figures. 2(b) and (c) show the energy dependence of the (1 0 0) and (0 0 1) reflections. Both exhibit only a $\sigma\rightarrow\pi'$ component, but their energy spectra are quite different. At the (1 0 0), three large resonant peaks at 4.974, 4.986, and 4.999 keV are observed, while at the (0 0 1) two large peaks are observed at 4.972 and 4.984 keV. At the pre-edge energy, a small resonant peak was observed at both reflections.[20] At the (011), both scattering components, $\sigma\rightarrow\sigma'$ and $\sigma\rightarrow\pi'$, were observed simultaneously as shown in Fig. 2(d). Both the components show the same energy dependence, exhibiting two large resonant peaks at 4.975 and 4.986 keV and a weak peak at the pre-edge. The precise energy dependence of the $\sigma\rightarrow\pi'$ component was also measured around the pre-edge feature as shown by the small filled circles in Fig. 2(d). In each of the reflections, several resonant peaks are observed above the main edge. In con-

TABLE I. The obtained parameter c_1 of the wave function, which is c_1zx+c_2xy ($c_1^2+c_2^2=1$) at site 1. The results have been determined by some theories, previous experiments (polarized neutron scattering and NMR), and our study.

	Theory	Neutron	NMR	Present result
c_1	~0.8 (Ref. 14), ~0.71 (Ref. 15)	~0.77 (Ref. 16)	~0.8 (Ref. 17)	~0.71

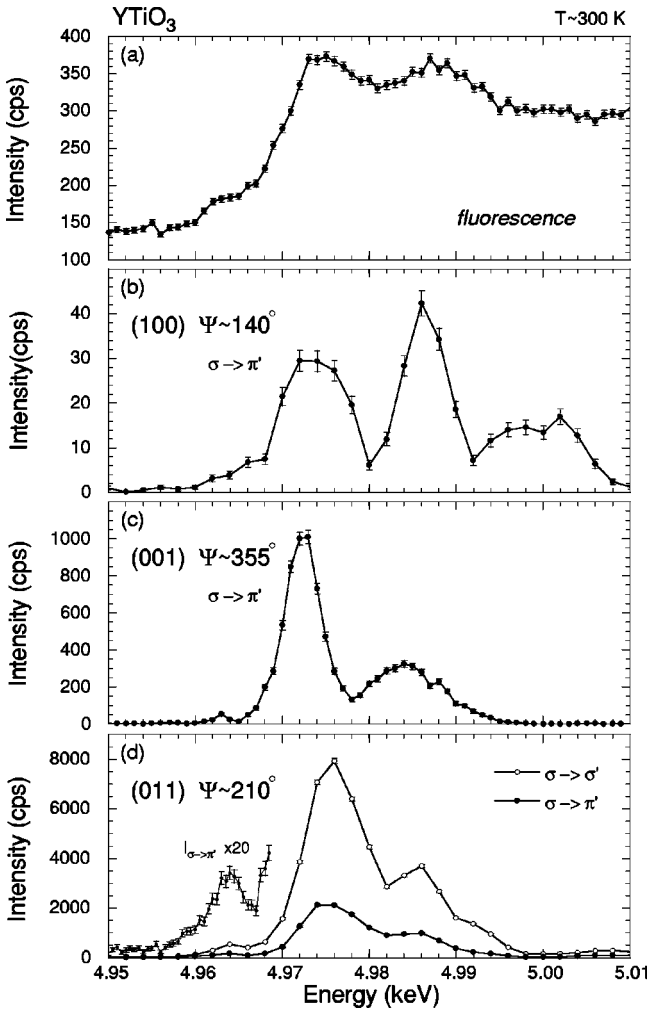

FIG. 2. (a) Fluorescence at (0,0,1.5) near Ti *K*-edge energy. (b)–(d) Energy dependence of RXS intensities at forbidden reflections. The scattering components, $\sigma \rightarrow \sigma'$ and $\sigma \rightarrow \pi'$, are shown by open circles and filled circles, respectively.

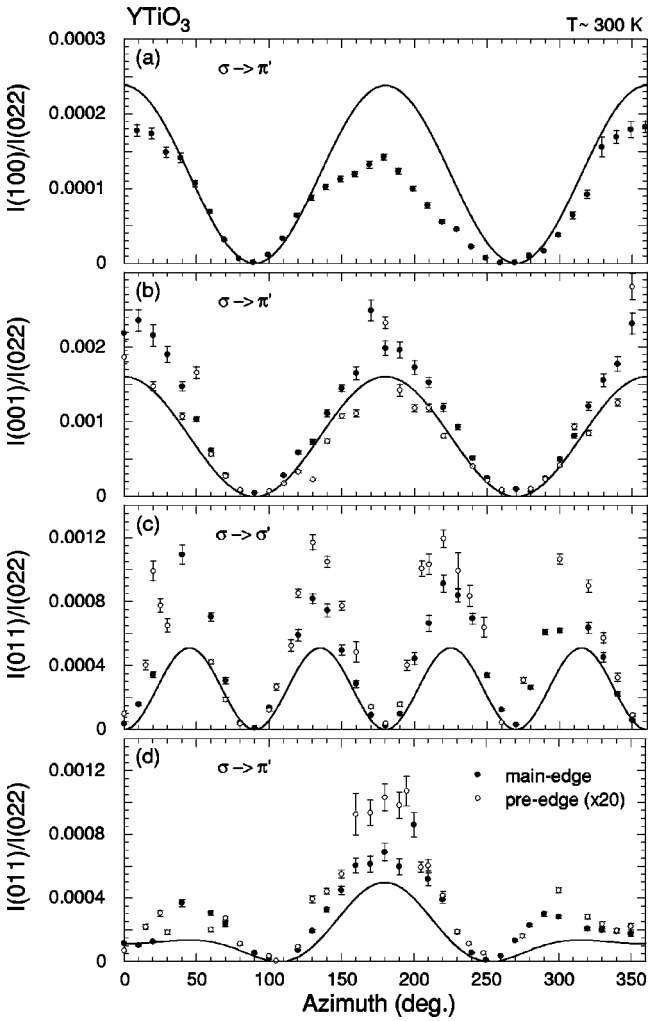

FIG. 3. Azimuthal angle dependence of the RXS intensities at (1 0 0) [(a)], (0 0 1) [(b)], and (0 1 1) [(c) and (d)]. The intensities at main edge are shown by filled circles, and those at pre-edge multiplied by 20 are shown by open circles. The Ψ of azimuthal angle is defined as follows: (a) and (b), $\Psi = 0$ at $\sigma \| b$; (c) and (d), $\Psi = 0$ at $\sigma \| a$.

trast, strong RXS was observed at only one resonant energy (main edge) in the manganite systems.[1,2] These energy dependences in $YTiO_3$ are, however, remarkably similar to the case of YVO_3.[9] The energies of the resonant peaks depend on the reflections, i.e., there is a large *Q*-position dependence. Nevertheless, the intensity ratio between the pre-edge and the main edge is almost constant, that is, $I_{pre}:I_{main} \sim 1:20$ without correction for absorption effects.

B. Azimuthal angle dependence

An important feature of resonant scattering is that, unlike nonresonant charge scattering, the intensity depends on the azimuthal angle, that is, rotating a sample about the scattering vector, provides direct information on the tensor of ASF. We have therefore measured the azimuthal angle dependence of the intensities at the forbidden reflections at the main edge. At each azimuthal angle, $\theta - 2\theta$ scans were performed. The resulting integrated intensities at (1 0 0), (0 0 1), and (0 1 1) were normalized by that of the fundamental peak of (2 0 0), (0 0 2), and (0 2 2), respectively, to correct for any variations due to a sample shape. The structure factors of the fundamental peaks were calculated by the crystal parameters in Ref. 13. Then, the results finally normalized by the intensity of (0 2 2) as a standard are shown by filled circles in Figs. 3. The azimuthal angle dependence of the (1 0 0) and (0 0 1) reflections exhibit twofold symmetry [Figs. 3(a) and (b)]. At the (0 1 1) reflection, the azimuthal angle dependence of the $\sigma \rightarrow \sigma'$ component shows a fourfold symmetry, while the $\sigma \rightarrow \pi'$ component has a period of 360°, as shown in Figs. 3(c) and (d), respectively. We have also measured the azimuthal angle dependence of the (001) and (011) reflections at the pre-edge, and found it to be the same as that at main edge, as shown by open circles in Figs. 3. The intensities were also normalized by the fundamental peak at main edge. In quantitative discussion, we need a correction for the energy dependence of the fundamental peak intensity.

C. Model calculation

The origin of the RXS at the main edge lies in the splitting of the Ti $4p$ energy levels. As a result, the ASF becomes a tensor rather than a scalar. As discussed above, the origin of this splitting remains controversial. However, on the basis of the two pictures proposed to date — namely the Coulomb mechanism and the JT mechanism—one can construct the tensor and make comparisons with our data.

In the case of the Coulomb mechanism, the Ti $4p$ energy levels are split by the on-site Coulomb interaction between the ordered $3d$ orbital and the $4p$ orbital of the Ti ion. The wave function, c_1zx+c_2xy, of the ordered orbital is expected at site 1, as shown in Fig. 1. The wave function is represented by xz' by definition, if we exchange the principal axes based on xyz coordinates for those based on $xy'z'$ coordinates, namely, the t_{2g} orbital is elongated in the xz' plane and not in the y' direction. Because of the on-site Coulomb interaction, then, the $4p_{y'}$ energy level is lowered and the $4p_x$ and $4p_{z'}$ are raised. The tensor at site 1 can be described as follows:

$$\begin{pmatrix} f_a & 0 & 0 \\ 0 & f_a+\Delta f_a & 0 \\ 0 & 0 & f_a \end{pmatrix} \text{ in the } xy'z' \text{ coordinates,}$$

where Δf_a is the anisotropic strength of ASF and f_a is the isotropic term. The angle between the z and z' axes following a rotation about the x axis is defined as r_x. We may thus describe the tensor with only two parameters, r_x and Δf_a. The tensors at the other three sites are also determined in the same way. These tensors satisfy the space group of the crystal structure, $Pbnm$. If the tensors do not satisfy the space group, the azimuthal angle and polarization dependences calculated from such tensors are completely different from the present experimental results. Thus the restriction of the space group is very strict. Moreover, sites 1–4 have different xyz coordinates due to the tilt of TiO_6 octahedra as a result of the $GdFeO_3$-type structural distortion. In our model calculation, the distortion is properly taken into account through the difference of the xyz coordinates among the sites. On the basis of these tensors, we can calculate the structure factor. The calculated $\sigma\rightarrow\pi'$ components of the intensity at each reflection with $\Psi=180°$ as a function of r_x are shown in Fig. 4. The intensity ratio among the RXS peaks depends strongly on the value of r_x. The experimentally observed RXS intensities are also plotted on the right ordinate in the figure. In the model calculation, the range of r_x for which the order among the RXS intensities is as observed is $30°-70°$. By comparing the measured intensity ratio among the RXS peaks with the calculated value, we find that $r_x=45\pm10°$, which is denoted by an arrow in Fig. 4. We can then use the value of $r_x=45°$ to calculate the azimuthal and polarization dependence of the three reflections. The results of these calculations are shown by the solid lines in Figs. 3. The agreement is fairly good. Thus the azimuthal angle and polarization dependence, and the intensity ratio among the RXS peaks, are explained by this model calculation which is based on the Coulomb mechanism. We conclude that the parameters of wave function of Ti $3d$ orbital, c_1 and c_2, are $c_1=0.71\pm0.11, c_1^2+c_2^2=1$. These are in good agreement with previous theories and experiments within our experimental error bar as shown in Table I.[14–17]

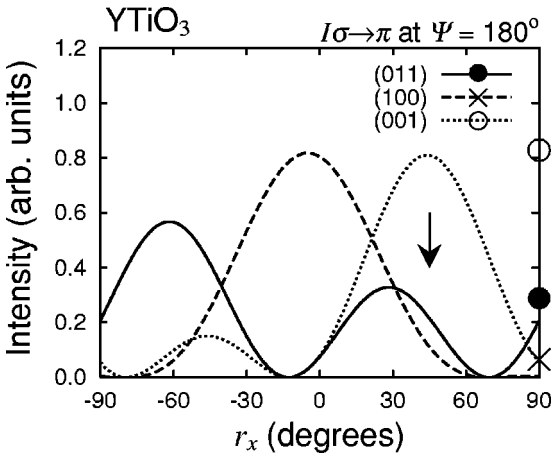

FIG. 4. The calculated rotation angle, r_x, dependence of the RXS intensities of $\sigma\rightarrow\pi'$ component at the azimuthal angle $\Psi=180°$. The relative intensities obtained from the experiments are plotted on the right ordinate.

In the case of the JT mechanism, the splitting of the $4p$ energy levels arises as a result of the oxygen motion that distorts the octahedron surrounding the Ti ion in the orbitally ordered state. The tensor is then that of the Coulomb mechanism without rotations, i.e., $r_x=0$ ($c_2=0$). It is obvious that $r_x=0$ required by this simplest version of the JT mechanism cannot explain our results. However, not only the JTD effect but also the effect of the neighboring octahedra may be considered as the origin of the RXS, as discussed in a theory.[18] We will return to this point below.

The anisotropic strength of the tensor, Δf_a, determines the intensity ratio between the RXS peak and the fundamental peak, while r_x controls the intensity ratio among the RXS peaks. By comparing the RXS and the fundamental intensities, we determined Δf_a to be 1.3 ± 0.1;[21] this value is also used for the solid curves shown in Figs. 3. We note that this value of Δf_a is larger than that of $LaMnO_3$ ($\Delta f_a\sim0.3$),[22] even though the JTD is smaller in $YTiO_3$ than that in $LaMnO_3$.

Next, we discuss the RXS intensity at the pre-edge. In principle, this intensity is theoretically expected to reflect the $3d$ orbital state directly, although the precise scattering mechanism is not well understood. In $LaMnO_3$, Elfimov *et al.* have performed LSDA+U calculations, which predict RXS due to a weak dipole transition, arising from the hybridization of the Mn $4p$ with the neighboring orbitally ordered Mn $3d$'s.[7] Takahashi *et al.* have also done similar discussion.[23] In V_2O_3, on the other hand, strong RXS is observed at pre-edge owing to the broken local inversion symmetry and that at main edge is not observed.[24] In this $YTiO_3$, the azimuthal angle, polarization, and Q-position dependence at the pre-edge are the same as those at the main edge, and there is inversion symmetry. Therefore the RXS at the pre-edge probably arises from a dipole transition, caused by the hybridization of the Ti $4p$ with the neighboring orbit-

ally ordered Ti $3d$'s. The ratio between the intensities at the pre-edge and at the main edge is almost independent of the reflection, within the experimental error. As a result, we can immediately determine $r_x \sim 45°$ at the pre-edge. The value, $\Delta f_a \sim 0.2$, at the pre-edge was also obtained by comparing the RXS and fundamental intensities with correction for absorption effect. Thus the tensor of ASF at the pre-edge has quantitatively been determined.

The tensors at a Ti site resulting from the JT mechanism and the Coulomb mechanism used in our model calculation are the JTD and a simple linear combination of two t_{2g} orbitals, respectively. Thus we have only examined as to which of these mechanisms is more significant in giving rise to RXS. The present observations are supportive of the model of Coulomb mechanism. Ishihara *et al.* have derived a general form for the scattering cross section of RXS and approached our results as a linear combination of three t_{2g} orbitals.[19] The determined parameters of wave function are better to fit for our results than our simple model calculation. On the other hand, Takahashi *et al.* have investigated the intensities of RXS at forbidden reflections using a band-structure calculation combined with the local-density approximation.[18] The calculated RXS intensities arise from not only the JTD but also the tilts of the neighboring TiO_6 octahedra. In our model of JT mechanism, only the tilt of the octahedra at the site where the x ray is absorbed is considered, but the tilts of the neighboring octahedra are not. The energy spectra obtained theoretically are similar to our experimental results, while the intensity ratio cannot be explained by this theory. In their paper, the Coulomb effect is not small, though it is less than 1/4 of JTD. The RXS intensity due to the Coulomb mechanism should be combined with their theory. Moreover, their model leads to a metallic ground state without orbital order. Therefore the experimentally observed RXS intensities at the pre-edge cannot be reproduced by their theory. The theoretical calculation of the LSDA+U method, which can handle orbital polarization easily, is strongly desired now.

D. Temperature dependence

To make clear the relationship among the crystal structure, the orbitally ordered state, and the RXS through T_c, the temperature dependence of the RXS intensity has been measured. It may reveal a coupling between the magnetism and the orbital state. Figure 5 (a) shows the temperature dependence of magnetization, which indicates the ferromagnetic ordering below T_c. The temperature dependence of the lattice constant, a and c, was estimated from the measured scattering angle for the (2 0 0) and (0 0 2), respectively, as shown in Figs. 5(b) and (c). In the temperature region above T_c, the temperature dependences are fitted by Debye approximation as shown by solid line in the figures. The anomalous temperature dependence can easily be estimated by the extrapolation of the fitted lines. There is a clear anomaly owing to a magnetostriction below T_c, namely the lattice constant a contracts and c expands. The temperature dependence of RXS intensity at main edge is shown in Fig. 5(d). The dependence shows no anomaly at T_c, although the magnetostriction owing to a structural change has been observed. The RXS at pre-edge also has no anomaly at T_c.

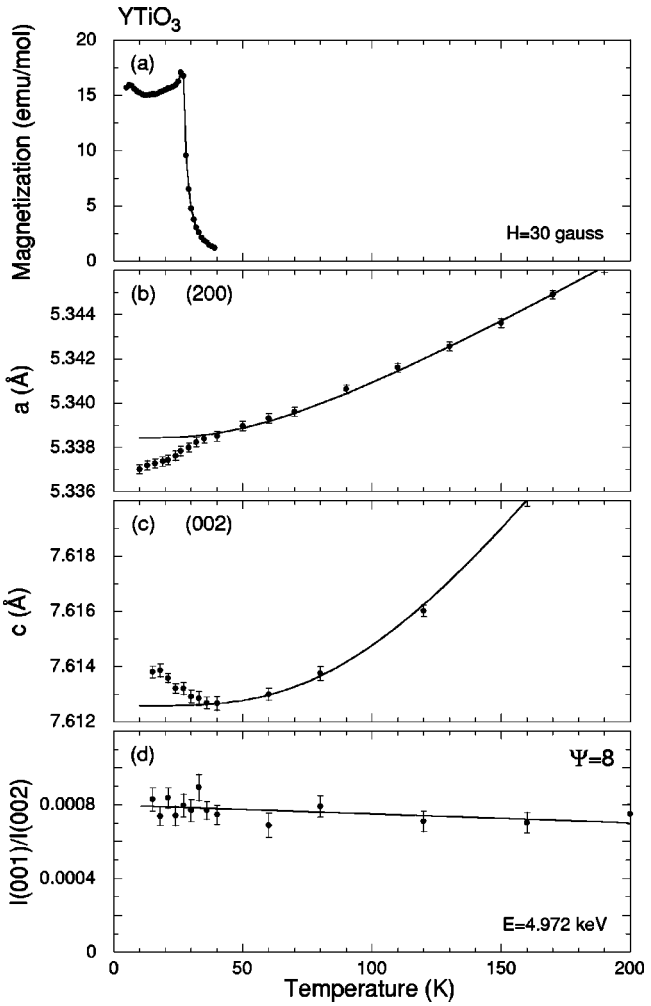

FIG. 5. Temperature dependence of the magnetization (a), lattice constant a (b), c (c), and RXS intensities at main edge (d).

We discussed a possible scattering scenario of the RXS here, namely Coulomb mechanism, JT mechanism and also other crystal structural mechanism. In any case, the coupling between RXS and magnetism is weak. In $Pr_{1-x}Ca_xMnO_3$,[5] the clear change has not been observed, while the notable temperature dependence has been observed at the magnetic transition in $KCuF_3$.[25] These results are interesting to consider not only the relationship between RXS and physical properties but also the scattering mechanism. Further experimental examples are required to understand it.

IV. CONCLUSION

We have utilized resonant x-ray scattering techniques to study the orbital ordering of the Ti $3d$ electrons in $YTiO_3$. By studying the azimuthal and polarization dependences of three independent forbidden reflections, we have performed a quantitative determination of the tensor of ASF above T_c. On the basis of the tensors, we have examined as to which of the mechanisms is more significant in giving rise to RXS,

namely, our models of the JT mechanism and the Coulomb mechanism. The model of the Coulomb mechanism can explain our data at the main edge. The obtained wave function of the orbitally ordered state, i.e., the linear combination of two t_{2g} orbitals, is in good agreement with the order previously obtained below T_c. The temperature dependence of the RXS has also been measured through the magnetic transition. The dependence shows no anomaly at T_c, although the magnetostriction has been observed. In conclusion, our experimental results seem to support a Coulomb mechanism in the main edge, though other mechanisms may also have an effect on the RXS. These measurements give hints to the scattering mechanism responsible for the resonant enhancement in these t_{2g} materials, although further theoretical studies are very desirable now. Finally, this work illustrates the ability to quantitatively determine the anisotropic scattering tensor — a quantity of some interest in describing the electric and magnetic properties of these materials.

ACKNOWLEDGMENTS

The authors thank T. Arima, K. Hirota, M. Kubota, S. Maekawa, M. Takahashi, J. Igarashi, and M. Blume for fruitful discussions. This work has been carried out at the National Synchrotron Light Source, Brookhaven National Laboratory, which is supported by the U.S. Department of Energy, Division of Materials Sciences and Division of Chemical Science (Contact No. DE-AC02-98CH10886). This study was supported by a Grant-in-Aid for Scientific Research from the Ministry of Education, Sports, Science and Technology Development Organization (NEDO), and by Core Research for Evolutional Science and Technology (CREST).

*Present address: Graduate School of Science, Tohoku University, Sendai 980-8578, Japan.

†Present address: Department of Physics, Nagoya University, Nagoya 464-8602, Japan.

‡Present address: HASYLAB at DESY, Notkestrasse 85, D-22603 Hamburg, Germany.

§Present address: Institute for Materials Research, Tohoku University, Sendai 980-8577, Japan.

[1] Y. Murakami, H. Kawada, H. Kawata, M. Tanaka, T. Arima, Y. Moritomo, and Y. Tokura, Phys. Rev. Lett. **80**, 1932 (1998).

[2] Y. Murakami, J.P. Hill, D. Gibbs, M. Blume, I. Koyama, M. Tanaka, H. Kawata, T. Arima, Y. Tokura, K. Hirota, and Y. Endoh, Phys. Rev. Lett. **81**, 582 (1998).

[3] K. Nakamura, T. Arima, A. Nakazawa, Y. Wakabayashi, and Y. Murakami, Phys. Rev. B **60**, 2425 (1999); Y. Endoh, K. Hirota, S. Ishihara, S. Okamoto, Y. Murakami, A. Nishizawa, T. Fukuda, H. Kimura, H. Nojiri, K. Kaneko, and S. Maekawa, Phys. Rev. Lett. **82**, 4328 (1999).

[4] M.v. Zimmermann, J.P. Hill, D. Gibbs, M. Blume, D. Casa, B. Keimer, Y. Murakami, Y. Tomioka, and Y. Tokura, Phys. Rev. Lett. **83**, 4872 (1999); Y. Wakabayashi, Y. Murakami, I. Koyama, T. Kimura, Y. Tokura, Y. Moritomo, K. Hirota, and Y. Endoh, J. Phys. Soc. Jpn. **69**, 2731 (2000); Y. Wakabayashi, Y. Murakami, Y. Moritomo, I. Koyama, H. Nakao, T. Kiyama, T. Kimura, Y. Tokura, and N. Wakabayashi, *ibid.* **70**, 1194 (2001); C.S. Nelson, M.v. Zimmermann, J.P. Hill, Doon Gibbs, V. Kiryukhin, T.Y. Koo, S-W. Cheong, D. Casa, B. Keimer, Y. Tomioka, Y. Tokura, T. Gog, and C.T. Venkataraman, Phys. Rev. B **64**, 174405 (2001); J.P. Hill, C.S. Nelson, M.v. Zimmermann, Y.-J. Kim, D. Gibbs, D. Casa, B. Keimer, Y. Murakami, C. Venkataraman, T. Gog, Y. Tomioka, Y. Tokura, V. Kiryukhin, T.Y. Koo, and S.-W. Cheong, Appl. Phys. A: Mater. Sci. Process. **73**, 723 (2001).

[5] M.v. Zimmermann, C.S. Nelson, J.P. Hill, D. Gibbs, M. Blume, D. Casa, B. Keimer, Y. Murakami, C.-C. Kao, C. Venkataraman, T. Gog, Y. Tomioka, and Y. Tokura, Phys. Rev. B **64**, 195133 (2001).

[6] S. Ishihara and S. Maekawa, Phys. Rev. Lett. **80**, 3799 (1998).

[7] I.S. Elfimov, V.I. Anisimov, and G.A. Sawatzky, Phys. Rev. Lett. **82**, 4264 (1999).

[8] M. Benfatto, Y. Joly, and C.R. Natoli, Phys. Rev. Lett. **83**, 636 (1999); M. Takahashi, J. Igarashi, and P. Fulide, J. Phys. Soc. Jpn. **68**, 2530 (1999).

[9] M. Noguchi, A. Nakazawa, S. Oka, T. Arima, Y. Wakabayashi, H. Nakao, and Y. Murakami, Phys. Rev. B **62**, R9271 (2000).

[10] B. Keimer, D. Casa, A. Ivanov, J.W. Lynn, M.v. Zimmermann, J.P. Hill, D. Gibbs, Y. Taguchi, and Y. Tokura, Phys. Rev. Lett. **85**, 3946 (2000).

[11] K. Hirota, N. Oumi, T. Matsumura, H. Nakao, Y. Wakabayashi, Y. Murakami, and Y. Endoh, Phys. Rev. Lett. **84**, 2706 (2000).

[12] H. Nakao, K. Magishi, Y. Wakabayashi, Y. Murakami, K. Koyama, K. Hirota, Y. Endoh, and S. Kunii, J. Phys. Soc. Jpn. **70**, 1857 (2001); F. Yakhou, V. Plakhty, H. Suzuki, S. Gavrilov, P. Burlet, L. Paolasini, C. Vettier, and S. Kunii, Phys. Lett. A **285**, 191 (2001).

[13] J.P. Goral, J.E. Greedan, and D.A. Maclean, J. Solid State Chem. **43**, 244 (1982); David A. Maclean, Hok-Nam Ng, and J.E. Greedan, *ibid.* **30**, 35 (1979).

[14] T. Mizokawa and A. Fujimori, Phys. Rev. B **54**, 5368 (1996); T. Mizokawa, D.I. Khomskii, and G.A. Sawatzky, *ibid.* **60**, 7309 (1999).

[15] H. Sawada, N. Hamada, and K. Terakura, Physica B **237-238**, 46 (1997).

[16] H. Ichikawa, J. Akimitsu, M. Nishi, and K. Kakurai, Physica B **281-282**, 482 (2000); J. Akimitsu, H. Ichikawa, N. Eguchi, T. Miyano, M. Nishi, and K. Kakurai, J. Phys. Soc. Jpn. **70**, 3475 (2001).

[17] M. Ito, M. Tsuchiya, H. Tanaka, and K. Motoya, J. Phys. Soc. Jpn. **68**, 2783 (1999).

[18] M. Takahashi and J. Igarashi, Phys. Rev. B **64**, 075110 (2001).

[19] S. Ishihara, T. Hatakeyama, and S. Maekawa, Phys. Rev. B **65**, 064442 (2002).

[20] The RXS at (1 0 0) was also observed at pre-edge despite the shoulder of the RXS at main edge.

[21] This value was estimated without correction for any extinction effects.

[22] This is a rough estimation based on the model tensor of ASF in Ref. 2.

[23] M. Takahashi, J. Igarashi, and P. Fulde, J. Phys. Soc. Jpn. **69**, 1614 (2000).

[24] M. Fabrizio, M. Altarelli, and M. Benfatto, Phys. Rev. Lett. **80**, 3400 (1998); L. Paolasini, C. Vettier, F. de Bergevin, F. Yakhou, D. Mannix, A. Stunault, W. Neubeck, M. Altarelli, M. Fabrizio, P.A. Metcalf, and J.M. Honig, *ibid.* **82**, 4719 (1999).

[25] L. Paolasini, R. Caciuffo, A. Sollier, P. Ghigna, and M. Altarelli, Phys. Rev. Lett. **88**, 106403 (2002).